Thesis for the Degree of Licentiate of Engineering

Phase sensitive amplifiers for free-space optical communications

Ravikiran Kakarla

CHALMERS

Photonics Laboratory
Department of Microtechnology and Nanoscience
Chalmers University of Technology
Gothenburg, Sweden, 2018

Phase sensitive amplifiers
for free-space optical communications

Ravikiran Kakarla

Technical Report MC2 - 400
ISSN 1652-0769

Photonics Laboratory
Department of Microtechnology and Nanoscience
Chalmers University of Technology
SE–412 96 Göteborg
Sweden
Telephone: +46–(0)31–772 10 00

Printed by Chalmers Reproservice, Chalmers University of Technology
Göteborg, Sweden, 2018

Phase sensitive amplifiers for free-space optical communications

Ravikiran Kakarla
Photonics Laboratory
Department of Microtechnology and Nanoscience
Chalmers University of Technology

Abstract

The demand for high data rate free-space communications is increasing due to the planned future space exploration missions. In the next few years there is a need to increase the speed by 100 times according to NASA, and this necessitates that transmission systems operate at higher carrier frequencies. Optical communication systems are capable of handling hundreds of Gigabits per second data with a single light carrier and are suitable for high data rate space communication links. The sensitivity of the receiver is one of the key factors to achieve such high speed communication. Phase sensitive parametric optical amplifier (PSA) can amplify optical signals ideally without degrading the signal to noise ratio. Employing these as pre-amplifiers in free-space receivers can thus improve the sensitivity significantly.

In this thesis we investigate the prospects of implementing a PSA based receiver for free space links. We use a 10 GBd QPSK signal and a pump wave to generate the necessary idler wave at the transmitter. The three waves are sent through a free-space link where only loss is considered as the channel impairment. The transmitted pump power was much lower than the combined signal and idler wave powers which would otherwise impair the overall sensitivity. At the receiver, the received pump power is as low as -65 dBm whereas a combined signal and idler power of -50 dBm was needed to achieve a bit-error rate of 10^{-3}. The received low power pump was recovered using injection locking and a phase locked loop setup. Key results show that, the sensitivity can be improved by 3 dB with respect to an low noise figure erbium doped fiber amplifier (EDFA) based receiver.

Keywords: Phase sensitive amplifier, optical injection locking, sensitivity and noise figure

Publications

This thesis is based on the work contained in the following papers:

[A] R. Kakarla, K. Vijayan, A. Lorences-Riesgo, P.A. Andrekson, "High Sensitivity Receiver Demonstration Using Phase Sensitive Amplifier for Free-Space Optical Communication", *Proceedings of European Conference on Optical Communications(ECOC)*, Paper. Tu.2.E.3, 2017.

[B] R. Kakarla, J. Schröder, P.A. Andrekson, "Optical injection locking at sub nano-Watt powers", *accepted for publication in optics letters.*

A subset of this work was presented in

R. Kakarla, K. Vijayan, J. Schröder, P.A Andrekson, Phase noise characteristics of injection-locked lasers operated at low injection powers, *Proceedings of Optical Fiber Conference(OFC)*, Paper. M4G.2, 2018.

Acknowledgement

First of all I would like to thank my supervisors Prof. Peter Andrekson and Prof. Magnus Karlsson for accepting me as a PhD student. Special thanks to Prof. Peter for supervising and motivating me all these years. Samuel Olsson along with Prof. Peter deserves a thanks for choosing this research topic for me to do PhD. Abel Lorences Riesgo deserves a special thanks for teaching me how to implement PSA experimentally and everything for the first time and guiding me to write the first paper. Thanks to Jochen Schröder for taking on responsibility for supervising me after Abel left and also for teaching me presentation and writing skills, although I am still learning. I would like to thank Kovendhan for taking part in my first experimental work and also for all the interesting discussions we had. Mikael also deserves a special thanks for the discussions and suggestions, specially for pointing the mistakes we do with DSP sometimes. They were really helpful.

When it comes to life here, Nishan deserves a big thanks for making me feel comfortable in the office and cheering me up because I have never lived outside India where I don't know anyone. Thanks to Ayesha for being my first 'Telugu' friend here and for sharing all interesting home town stories. Shrey, Nimanand also deserves thanks for making me drink first alcoholic drink in my life and teaching me some wisdom. Last but not the least, I would like to thank my parents, sister and brother-in-law for all the support and care.

Ravikiran Kakarla

This work has been financially supported by Swedish research council (VR), European research council (ERC) and Wallenberg foundation (KAW).

Contents

Acronyms

APD	Avalanche photo detector
ASE	Amplified spontaneous emission
BPSK	Binary phase shift keying
DFB	Distributed feedback laser
EDFA	Erbium doped fiber amplifier
FEC	Forward error correction
FWM	Four-wave mixing
GEO	Geostationary orbit
HNLF	Highly nonlinear fiber
ILIP	Injection locking induced pulsations
LDPC	Low density parity check codes
LLCD	Lunar laser communication demonstration
LO	Local oscillator
NF	Noise figure
OIL	Optical injection locking
OSNR	Optical signal to noise ratio
PLL	Phase locked loop
PMT	Photomultiplier tube
PPB	Photons-per-bit
PPM	Pulse position modulation
PSA	Phase sensitive amplification
PZT	Piezoelectric transducer
QPSK	Quaternary phase shift keying
RF	Radio frequency
SNR	Signal to noise ratio
WDM	Wavelength division multiplexing

Chapter 1

Introduction

Future expeditions into deep space require fast and efficient ways of communication with earth. To accomplish such missions, streaming of high definition videos, images and data transmission in real time across the deep-space are necessary. This necessiates the state-of-the-art communication technology to perform 100 fold faster and more efficient than today [1, 2]. Current state-of-the-art radio frequency (RF) technology for deep-space communication that operates in the Ka band (26 GHz - 40 GHz) has been introduced to replace previous generation X-band frequency (1 - 10 GHz) for space missions such as Mars Reconnaissance orbiter (MRO) 2005, Cassini at Saturn, 2004, due to increase demand for high information rates [2]. Future missions involving high speed data transmission creates a bottleneck when using RF communications. Free-space optical communications uses light as carrier wave with frequency 10^4 times higher than the RF, allowing data transmission at higher data rates. Lunar laser communication demonstration (LLCD) was the first attempt of such a feat by NASA, sending a satellite with laser based transciever to the moon operating at around 1550 nm wavelength with 622 Mbps downlink rate to communicate to earth [3]. This demonstration in 2013 paved the way to upcoming missions include laser communication to Mars by 2020 and high speed near earth communication such as laser communication relay demonstration (LRCD) for downloading multi-tera bytes of data per day from outer space satellites as well as high speed communication within the network of relay in GEO and ground station as shown in Fig. 1.1 [4].

On the contrary, communication from long distance planets for example, Saturn situated at 1 billion kilometers from earth could be extremely difficult because of the power budget, defined as the allocated transmitted

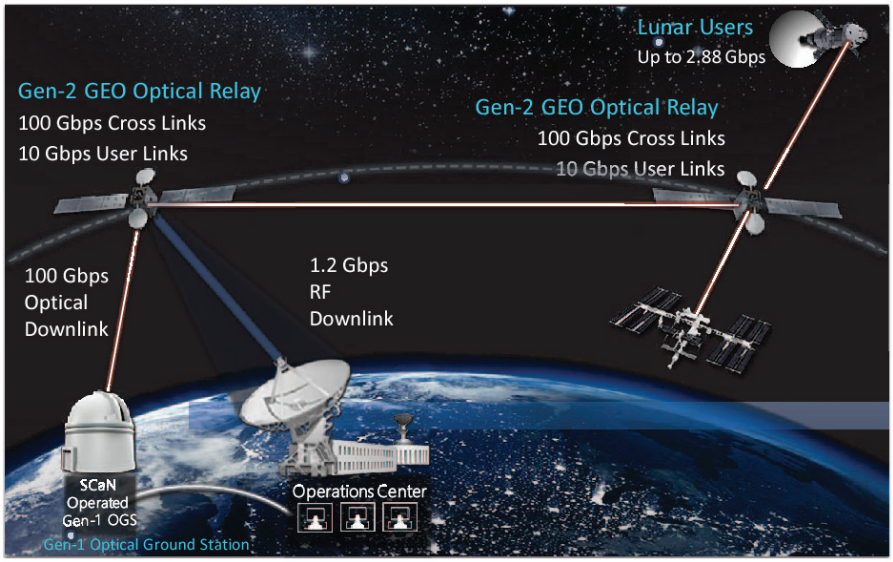

Figure 1.1: NASA relay constellation in 2025 [4]

power for reliable communication considering all the losses in the channel, for such long distances may be too large for practical implementation. In other words, systems that can transmit 10 Gbps data from GEO orbit to ground station may only achieve 10 bps from Saturn. Increasing the power efficiency by choosing appropriate modulation format, forward error codes (FEC) and high sensitive receiver will improve the power budget [1]. Having implemented these technologies, one could achieve nominal data rates only upto 6 Mbps to Mars in MRO 2006 and few hundred kbps to Saturn in Cassini 2004 [1].

Typical modulation formats used for free-space communications are pulse position modulation (PPM) and on-off keyed modulation along with powerful FEC such as turbo codes and low density parity check codes (LDPC). In the receiver side, low noise amplifier and large antennas were used [1].

Optical communication not only has higher carrier frequency but also exhibit lower beam divergence as beam divergence angle is proportional to wavelength allowing optical beams to be 10^4 times narrower than the RF beams. This means more power concentrated in smaller area making laser communication more power efficient than RF communication and also allowing smaller dimensions of the receiver antenna or detector. Of course, this places a requirement on precise beam alignment with receiver antenna which was accomplished in LLCD 2013.

Hence one could say that optical communication could be the optimal option to probe into deep-space to meet the requirements of high speed next

generation space communication technology. Optical transmitters and receivers are widely available at C-band (1530 - 1560 nm) and L-band (1560 -1625 nm) due to the well established fiber optic communication technology. As a matter of fact, the power efficient transmitter and receiver technologies can be adapted from fiber-optic communication technology but not necessarily with high spectral efficiency because the data rate will be much smaller than long haul fiber transmission (Typically > 1 Tbps).

The sensitivity of the free-space communication system can be improved by choosing modulation formats like PPM, polarisation switching, frequency shift keying (FSK) has been demonstrated in [5, 6] and also by using high sensitive optical receivers or detectors. Most widely used optical receivers are single photon avalanche photodetectors (APDs), photon multiplier tubes (PMTs) and nanowire detectors [7–9], however their available bandwidth is limited to few MHz. A pre-amplifier to the receiver can also be used to improve the receiver sensitivity. Typically erbium doped fiber amplifiers (EDFA) are used as pre amplifiers having a ideal noise figure (NF) of 3 dB. On the other hand, a phase sensitive amplifier (PSA) can ideally have a NF of 0 dB and employing such a pre-amplifier can thus improve the sensitivity by 3 dB or 100 percent power efficiency, is discussed in this thesis.

1.1 This work

In this work, we show the implementation of a phase sensitive amplifier as a pre-amplifier for a free-space communication receiver where the received power levels are extremely low. Unlike EDFA, PSAs require additional waves at the input, namely the idler (conjugate of signal) and the pump wave. To achieve the 3 dB sensitivity advantage, the pump power received needs to be recovered from powers typically below -65 dBm, which is here realised using optical injection locking (OIL) and a phase locked loop. In Paper(A), we implement phase sensitive amplifier for free space channel considering all the conditions mentioned above. We achieved 2.9 dB sensitivity improvement over conventional EDFA, measured at BER=10^{-3} 10 GBd QPSK signal. We also discuss the performance of PSA under the influence of atmospheric turbulence in the channel emulated in lab using a rotating phase screen plate. In Paper(B) we discuss in detail the implementation of OIL at -65 dBm using a PLL and a pre-amplifier. We also discuss its performance at low powers as it could affect the PSA sensitivity due to the phase noise generated in the OIL.

Chapter 2

Free-space optical communication

2.1 Free-space communication link

In a typical long haul free-space link, communication takes place between a deep space satellite and a communication receiver on earth or in the orbit around the earth, usually GEO. The satellite in the deep-space is usually the transmitter sending high speed data to the ground station or the satellite in the orbit which serve as a receiver. The schematic of free-space optical communication system is shown in the Fig. (2.1). [1]

The link consists of optical transmitter, free-space channel and optical receiver. The functions of the optical transmitter are to encode and modulate the information onto the optical carrier, provide appropriate optical power by amplifying the optical signal and provide necessary optical lens arrangement to point towards the receiver.

The signal passes through the optical channel which adds loss due to the divergence of the optical beam, inversely proportional to the link distance (R) square, $1/R^2$ [1]. The free-space channel also introduces

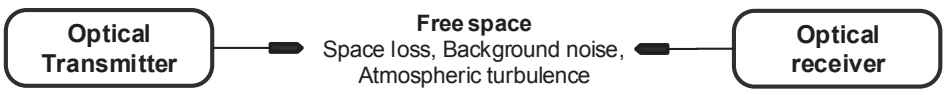

Figure 2.1: Free space communication link

background noises from the sun, moon and bright stars for deep-space links. If the earth terminal is ground based, the signal also passes through the earth's atmosphere which introduces sky irradiance, scintillations due to turbulence effects and attenuation due to clouds and rain etc.

The crucial function of the receiving terminal is to have appropriate receiver optics to receive the light with maximum efficiency and to provide sufficient sensitivity to receive signals, demodulate and decode the information. [1]

2.2 Link equation and received signal power

The performance of the optical link is decided by the signal power received, which is governed by the link equation [1]

$$P_s = P_t \left(\eta_T \frac{4\pi A_T}{\lambda_T^2} \right) L \left(\frac{A_R}{4\pi z^2} \right) \eta_R \tag{2.1}$$

where
P_s, P_t are received and transmitted signal power at input to receiver and at transmit antenna interface.
η_T, η_R are the transmitting and receiving optics efficiency
A_T, A_R are the aperture areas of transmitting and receiving optics
L is the loss in the channel due to the beam pointing inaccuracy
z is the link distance and $A_R/4\pi z^2$ is the fraction of power collected by receiving aperture considering transmitter is isotropic.
λ_T is the transmitted signal wavelength. Optical carrier wavelength (frequency, $f_{optical}$ = 200 THz) is much smaller compared to the RF (f_{RF}= 20 GHz). Hence the light beam diverges less than RF beam resulting higher received signal power (10^8 times) compared to RF.

According to the link equation Eq. (2.1), the received power can be increased by either

- Increasing transmitter power, but this might lead to an excess power consumption in the space crafts.
- Increasing the transmitter aperture, but size is correlated with mass and hence can not be increased indefinitely.
- Reducing operating wavelength of signal, but the unavailability of lasers and detectors at such wavelengths could be a drawback.
- Increasing receiver aperture area, but this can be useful for the case of the receiver being on the ground but the amount of background noise collected also increases with receiver aperture.

2.3 Optical receiver sensitivity

In the previous section, we have discussed ways to improve the received power in a free-space link which eventually improves the power budget. The performance of the link can also be improved by improving the receiver sensitivity (measured in photons/bit), is an important factor when designing a free-space communication link. There are different ways to improve the receiver sensitivity in a typical free-space link, are discussed below.

2.3.1 Detectors

There are two types of detectors can be used in receivers, coherent receivers or a direct detection receivers. In coherent receivers, incoming signal is beat with a strong local oscillator (LO) and the beat signal is detected in both quadratures using a pair of photo detectors. The local oscillator power is usually more than 10 mW and the received signal power in the range of micro watt or lower. Due to the beating of the strong LO with a weak signal, the noise level of signal increases much above the detector thermal noise. A coherent receiver is thus limited by shot noise of the signal and amplified spontaneous emission (ASE) induced beat noise if a pre-amplifier is used.

Whereas in a direct detection receiver, optical intensity is detected and it needs no processing steps that are required for coherent detection scheme. Direct detectors are usually limited by the detector thermal noise. According to reference [10], photon counting direct detection receivers can achieve higher sensitivity than coherent detection scheme by choosing appropriate modulation formats such as M-ary pulse position modulation (M-PPM). Photon detection efficiency can be improved in direct detection schemes such as avalanche photo diodes (APDs) and photo multiplier tubes (PMTs) where the current is multiplied many folds in the detector.

2.3.2 Pre-amplifier

A pre-amplifier is used to amplify the received signal and to the receiver sensitivity in the limit of high gain. For a pre-amplified receiver, the receiver noise is dominated by amplified quantum noise of the signal rather than the thermal noise of the detector. EDFAs are usually used for pre-amplification, which have a 3 dB quantum limited NF, meaning that the noise is amplified twice as the signal. Whereas in a phase sensitive amplifier, with ideal noise figure is 0 dB and thus can improve the sensitivity over an EDFA by 3 dB.

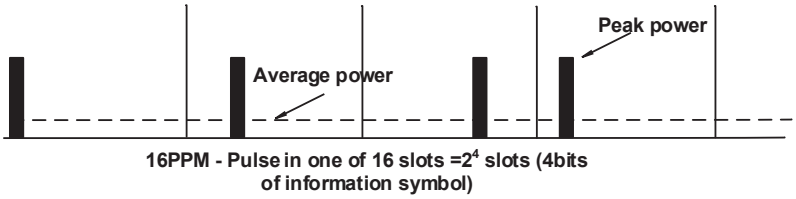

Figure 2.2: Example of Mary PPM with M=16

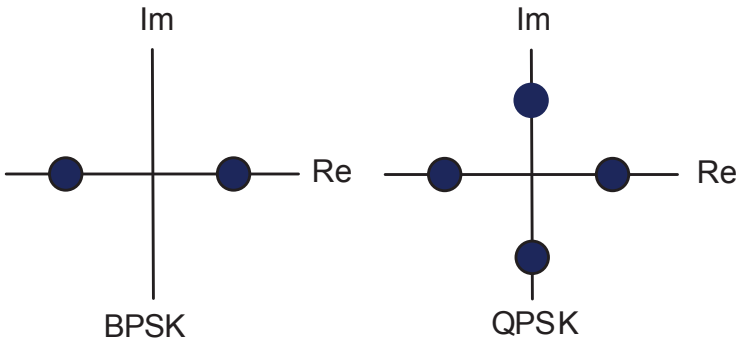

Figure 2.3: Constellation diagram of BPSK and QPSK

2.3.3 Modulation formats

Pulse position modulation format with direct detection is the most widely used modulation scheme for free-space/deep-space communications due to its theoretical capacity to reach Shannon's limit at sufficiently large peak to average ratio [1]. In a M-ary PPM modulation scheme each channel period symbol is divided into M time slots and the information is conveyed by the time window by which the signal pulse is present. An illustration of 16 PPM is shown in the Fig. 2.2

From the Fig. (2.2), to transmit 4 bits of information we need 16 time slots, but the power needed to be only in 1 slot. Since the information lies in the position, the power efficiency can be improved but at the expense of spectral efficiency.

Although PPM is a power efficient modulation format, its spectral efficiency is much lower compared to standard modulation formats for coherent communication like binary phase shift keying (BPSK) and quaternary

phase shift keying (QPSK). A simple BPSK and QPSK constellations are shown in Fig. 2.3 where the phase of the optical field is modulated, resulting in 1 and 2 bits per-symbol or per-time slot. In deep-space, where there is a need for both power efficient and high speed communication links, it is necessary to consider spectral efficiency along with power efficiency when choosing a modulation format.

2.3.4 Channel coding

To perform error free communication for long distances, there are constraints on the modulation formats due to their implementation using physical devices. For example PPM enforces constraints on the relative location of pulses and describes the mapping of bits to the sequence of pulses. For example Q-switched laser used as transmitter require a minimum delay between the pulses. These constraints can limit the performance especially in higher order PPM [1].

On the other hand forward error correction (FEC) codes with soft decision decoding can achieve the Shannon's capacity limits. FEC adds redundancy to the transmitted information using a pre determined algorithm. The redundant bits are complex functions of original information bits. This technique enhances the data reliability and error free communication. Typical FEC codes used for free-space communication are turbo codes and LDPC codes. [1]

2.4 Atmospheric channel

A free-space communication channel especially for deep space links, can be assumed as a simple lossy channel with a loss inversely proportional to square of the distance. For communications within the earth atmosphere, atmospheric turbulence and visibility severely affect the link performance [11]. Atmospheric turbulence creates beam vandering (changing direction of the beam) and scintillations resulting in phase and amplitude fluctuations in the wave front which obey Kolmogorov statstics of turbulence [12]. This leads to amplitude and phase fluctuations in the received signal. The refractive index fluctuations seen by the optical beam due to atmospheric turbulence is characterized by a parameter called atmospheric structure constant of refractive index C_n^2. This phase distortion is quantified by a parameter called Rytov variance given by the expression [12]

$$\sigma^2 = 1.23 C_n^2 (2\pi/\lambda)^{7/6} L^{11/6} \tag{2.2}$$

where L is the length in meters and λ is the wavelength. Rytov approximation predicts that the fluctuations can increase monotonically with link length.

2.4.1 Turbulence phase plate

The effects of turbulence can be emulated by a rotating phase screen plate in the laboratory environment. The random phase distribution obeying Kolmogorov statistics and characterized by effective Fried coherence length (Spatial) r_0 was machined on the plate. The parameter r_0 is defined as the diameter of wavefront area over which rms phase variations due to turbulence equal to 1rad. If the beam size is much larger than the r_0 value, we can consider that the effect of turbulence on the beam is minimal and vice versa.

The strength of the atmospheric turbulence is varied by varying r_0 value. [13, 14] The atmospheric structure constant for a phase plate is given by

$$C_n^2 = 2.36(\lambda/2\pi)^2(r_0)^{-5/3} \tag{2.3}$$

and the corresponding Rytov variance

$$\sigma^2 = 0.56C_n^2(2\pi/\lambda)^{7/6}(0.25L)^{5/6} \tag{2.4}$$

To relate the parameters of the simulated link to the real atmosphere, it is required that the Rytov varience of practical atmospheric link Eq. 2.2 should be equal to the estimated lab link Eq. 2.4 [13, 14]. The design parameter r_0 for the phase plate, describing the amount of turbulence induced within the beam is chosen to match the real atmospheric turbulence over a desired distance. In paper (A), we discuss the emulation of atmospheric turbulence using a phase plate with a r_0 values 0.3mm, 0.8mm and 2mm for high, medium and low turbulence for a 1 km real atmospheric link.

Chapter 3

Phase sensitive amplifier

Phase sensitive amplifiers (PSAs) are known for low noise amplification of optical signals, ideally addition adding no noise (NF = 0 dB) whereas the conventional EDFAs can have NF theoritically 3 dB. EDFAs operate on electronic transitions between energy levels whereas PSAs operate by the parametric amplification and coherent addition of optical signals due to the nonlinear phenomenon such as four-wave mixing or sum/difference frequency generation [15–19].

PSAs were first conceptualized in the year 1982 [20], where the author shows that there exists a bandwidth dependent lower limit on the noise carried by one quadrature of signal i.e., 0 dB if two modes are considered as inputs. This was first experimentally demonstrated in χ^2 material [21] then using χ^3 material using a nonlinear fiber [22]. Later PSAs were considered for different possible configurations for a fiber [23] and soon later it has been realized in real fiber optic communication environment [24] used as inline amplifier. It has also been used as regenerator for fiber transmission links by squeezing the phase and amplitude noise [25]. Recent demonstrations show that, PSAs can be used to reach 6 times more transmission distance compared to EDFA [26]. In this thesis we show the prospects of using PSA as high sensitive pre-amplifier for receiver in free-space communications due to the 3 dB benefit of noise figure over EDFA. Two main mechanisms behind the operation of PSA are the four-wave mixing and parametric amplification process in a χ^3 nonlinear medium.

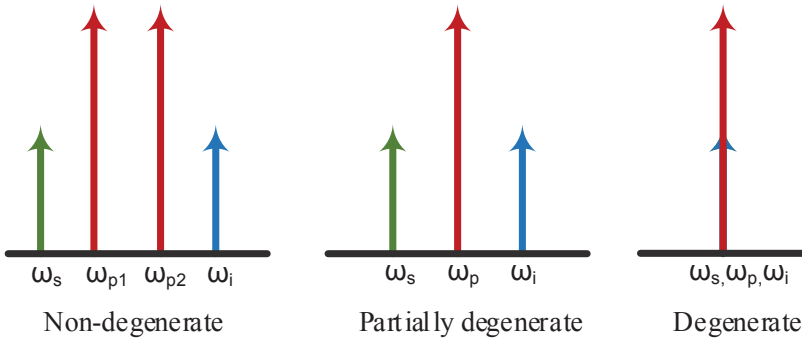

Figure 3.1: Four wave mixing schemes

3.1 Four-wave mixing

Four-wave mixing is a third order nonlinear phenomenon where three optical waves of different frequencies interact in a nonlinear medium to generate the fourth frequency by satisfying the laws of energy and momentum conservation [27]. If the three mixing frequencies are different, it is called non degenerate four-wave mixing and if two of the mixing frequencies are same, it corresponds to partially degenerate case and if all are same, it is called completely degenerate four-wave mixing [28]. The generated frequency is called as idler or conjugate or satellite [27]. The name conjugate is used because four-wave mixing is mostly used in partially degenerate case with a single pump and a signal interact to generate a conjugate of the signal. However the generated wave need not to be a conjugate of signal in general. The Fig. (3.1) show the classification of all the three configurations.

In this thesis, we study the partially degenerate case where a pump wave interact with a weaker signal to generate the idler wave. In order to satisfy the conservation of energy and momentum the frequency of pump related to signal and idler by $2\omega_p = \omega_s + \omega_i$ and propagation constant $2\beta_p = \beta_s + \beta_i$ where p, s, i are notations of pump, signal and idler. The generated idler power is proportional to the square of injected pump P_p^2, signal power P_s and the phase mismatch factor. The expression for idler power is given by [29]

$$P_i(L) = 4\eta_i\gamma^2 P_p^2 P_s e^{-\alpha L}\left(\left|\frac{1-e^{-\alpha L}}{\alpha}\right|^2\right) \tag{3.1}$$

where α, γ are the attenuation coefficients, nonlinear coefficient of the HNLF and η is the FWM efficiency, which depends on the phase mismatch

factor given by the Eq. 3.2 [30]

$$\eta = \left(\frac{\alpha^2}{\alpha^2 + \Delta\beta^2}\right)\left[1 + \frac{4e^{-\alpha L}\sin^2(\Delta\beta L)}{|e^{-\alpha L} - 1|^2}\right] \tag{3.2}$$

where $\Delta\beta = 2\beta_p - \beta_s - \beta_i$ is the phase mismatch factor, if $\Delta\beta = 0$, the FWM efficiency becomes 1 i.e., maximum. Due to dispersion in the HNLF the pump, signal and idler waves travel at different velocities, resulting in finite phase mismatch $\Delta\beta$ and hence the conversion efficiency is less than 1.

3.2 Parametric amplification

When a high power pump is launched into a HNLF, noise around the pump will start experiencing amplification as the energy of the pump gets transferred to higher and lower frequencies satisfying energy and momentum conservation. This can be assumed as FWM process under phase matching condition. If a weak signal wave is present instead of noise in the gain region, it will see an amplification and also generate a idler by FWM. The shape of the gain spectrum depends on the pump power and phase matching condition in the fiber. Parametric gain can be understood in more detail using the propagation equations for power of pump, signal and idler are obtained by substituting the fields of these waves in nonlinear Schrödinger equation and are given by Eq. 3.3 and Eq. 3.4 [31]

Note that the terms related to self-phase modulation and cross-phase modulation are ignored here.

$$\frac{dP_p}{dz} = -4\gamma(P_p^2 P_s P_i)^{1/2}\sin\theta \tag{3.3}$$

$$\frac{dP_s}{dz} = \frac{dP_i}{dz} = 2\gamma(P_p^2 P_s P_i)^{1/2}\sin\theta \tag{3.4}$$

and

$$\frac{d\theta}{dz} = \Delta\beta + \gamma(2P_p - P_s - P_i) + \left(\sqrt{\frac{P_p^2 P_s}{P_i}} + \sqrt{\frac{P_p^2 P_i}{P_s}} + 4\sqrt{P_s P_i}\right)\cos\theta \tag{3.5}$$

where $\theta = \phi_p - \phi_s - \phi_i$.

ϕ_p, ϕ_s and ϕ_i are the absolute phases of pump, signal and the idler. In Eq. (3.3) and Eq. (3.4), the negative and positive sign on the right hand

side indicate the pump power is attenuated and the signal and idler being amplified as they propagate in the fiber. This transfer of energy depends on the relative phase value θ and should ideally $\pi/2$ to have maximum energy transfer form pump to signal and idler.

If $\theta = \pi/2$ in the Eq. 3.5, the last term will be zero and to stay phase matched we need

$$\kappa = \Delta\beta + \gamma P_p = 0 \tag{3.6}$$

Assuming the pump power is much higher than the signal and idler power.

It is clear from Eq. 3.6 that in order to have perfect phase matching, $\Delta\beta$ should be negative. If the pump frequency is close to zero dispersion frequency of the HNLF ω_0 which is a practical case, then the phase matching condition can be written as

$$\kappa = \beta_3(\omega_p - \omega_0)(\omega_s - \omega_p)^2 + \gamma P_p = 0 \tag{3.7}$$

Here β_3 is the third derivative of the propagation constant at ω_0. Eq. 3.7 shows that, to have the phase matching condition condition satisfied the difference $\omega_p - \omega_0$ must be negative. In other words, pump frequency should be in the anomalous dispersion regime, to have maximum parametric gain. Assuming no pump depletion and a for weak signal injected, the analytical solutions for the signal gain is given by

$$G = \left(1 + \frac{\gamma P_p}{g}\sinh(gL_{eff})\right)^2 \tag{3.8}$$

where L_{eff} is the effective length of the fiber defined by $L_{eff} = [1 - e^{-(\alpha L)}]/\alpha$ and g is the parametric gain coefficient given by

$$g = \left[(\gamma P_p)^2 - \left(\frac{\kappa}{2}\right)^2\right] \tag{3.9}$$

Under perfect phase matching case $\kappa = 0$ the expression for signal gain can be simplified to

$$G = \frac{1}{4}\exp(2\gamma P_p L_{eff})) \tag{3.10}$$

From the Eq. 3.10 we can infer that, the signal will grow exponentially with respect to the pump power if the phase matching condition is satisfied. This gain region is also called as exponential gain regime due to the exponential dependence of gain on the pump power. The gain dependence on pump power can become quadratic if signal wavelength is close

to the pump. However, this condition is not relevant for discussion in this thesis as we operate in exponential gain regime. The maximum amount of pump power is limited by the brillouin scattering threshold, the power level above which pump will start reflecting back due to acoustic phonon vibrations in the HNLF.

3.3 Phase sensitive amplification - Transfer matrix approach

Equations (3.8) and (3.9) describe the gain of parametric amplifier where input is signal wave. If one wish to study the phase sensitive case, where a non zero idler also present at the input, we need a more sophisticated model to understand the process. A transfer matrix describing the fields of signal and idler at output of parametric amplifier in terms of input fields is given as

$$\begin{bmatrix} B_s \\ B_i \end{bmatrix} = \begin{bmatrix} \mu & \nu \\ \nu^* & \mu^* \end{bmatrix} \begin{bmatrix} A_s \\ A_i^* \end{bmatrix} \tag{3.11}$$

The matrices A and B are correspond to the input and output of the parametric amplifier. s and i denotes signal and idler waves. super script * denotes the complex conjugate. μ and ν are the complex transfer coefficients approximately given by.

$$\mu = \cosh(gL) - i\frac{\kappa}{2g}\sinh(gL) \tag{3.12}$$

$$\nu = i\frac{\gamma P_p}{2g}\sinh(gL) \tag{3.13}$$

However, it is important that μ and ν satisfy the relation [32]

$$|\mu|^2 - |\nu|^2 = 1 \tag{3.14}$$

From Eq. (3.11) the output signal is obtained by coherent addition of input signal and idler conjugate multiplied by their coefficients μ and ν. Rewriting the interacting fields in terms of powers by considering $A = \sqrt{P}e^{j\phi}$, the signal gain is obtained as

$$G_{PSA,s} = \frac{|B_s|^2}{|A_s|^2} = |\mu|^2 + \frac{|\nu|^2 P_{i0}}{P_{s0}} + 2|\mu||\nu|\sqrt{\frac{P_{i0}}{P_{s0}}}\cos(\phi_\mu + \phi_\nu + \theta_{rel}) \tag{3.15}$$

Here P_{i0}, P_{s0} are input idler and signal powers. $\phi_{\mu,\nu}$ denote the phase angles of the complex transfer coefficient and we have introduced the relative phase $\theta_{rel} = \phi_s + \phi_i$, is the phase angle measured relative to the pump. For zero input idler power, the gain is simply $|\mu^2|$ and is the phase in-sensitive parametric gain denoted by G earlier in Eq.(3.8)

The maximum achievable PSA gain in Eq.(3.15) is

$$G_{PSA,s} = \frac{(\sqrt{GP_{s0}} + \sqrt{(G-1)P_{i0}})^2}{P_{s0}} \tag{3.16}$$

$$G_{PSA,i} = \frac{(\sqrt{GP_{i0}} + \sqrt{(G-1)P_{s0}})^2}{P_{i0}} \tag{3.17}$$

It can also be shown that, the PSA minimum gain is $1/G_{max}$ which means PSA can attenuate by the same factor as it can amplify. When input signal and idler have identical power, phase sensitive gain will be 4 times the in-sensitive gain $G_{PSA,s} = 4G$

3.3.1 Noise figure

Until now we have assumed signal without any noise. In reality, PSA is limited by quantum noise, which is also considered as zero point energy or vacuum energy given by $h\nu/2$ at a given frequency ν. Quantum noise can be statistically expressed similar to additive Gaussian noise. Quantum noise is considered to be uncorrelated at all frequencies, thus $\langle n_s n_i \rangle = 0$, $\langle n_s \rangle = 0$ and $\langle |n_s|^2 \rangle = h\nu/2$. where $\langle . \rangle$ is the expectation operator and n_s, n_i are noises at signal and idler. Transfer matrix model is now written as

$$\begin{bmatrix} B_s \\ B_i \end{bmatrix} = \begin{bmatrix} \mu & \nu \\ \nu^* & \mu^* \end{bmatrix} \begin{bmatrix} A_s + n_s \\ A_i^* + n_i^* \end{bmatrix} \tag{3.18}$$

Since n_s and n_i are the uncorrelated, the amplification of noise will be $|\mu|^2 + |\nu|^2$. We know that the gain of PIA be $G = |\mu|^2$, we can thus write the noise gain $G_{noise} = |\mu|^2 + |\nu|^2 = 2G - 1$. Noise figure can be written as

$$NF = (SNR_{in})/(SNR_{out}) = G_{noise}/G_{sig} \tag{3.19}$$

substituting the expressions for signal gain and noise gain in the Eq. 3.19, for phase in-sensitive amplifier

$$NF_{PIA} = \frac{2G-1}{G} \tag{3.20}$$

and for phase sensitive amplifier

$$NF_{PSA_s} = \frac{(2G-1)P_{s0}}{(\sqrt{GP_{s0}} + \sqrt{(G-1)P_{i0}})^2} \tag{3.21}$$

$$NF_{PSA_i} = \frac{(2G-1)P_{i0}}{(\sqrt{GP_{i0}} + \sqrt{(G-1)P_{s0}})^2} \tag{3.22}$$

In the approximation $G >> 1$ which is practical case, $NF_{PIA} = 2$ (3 dB) and $NF_{PSA} = 1/2$ (-3 dB). Since PSA has both signal and idler as inputs, we need to account for idler power also. The combined noise figure for PSA will be

$$NF_c = NF_s + NF_i = NF_s \frac{P_{s0} + P_{i0}}{P_{so}} \tag{3.23}$$

This means that the combined noise figure is approximately equal to summation of signal and idler noise figures. If $P_s = P_i$ then the $NF_c = 1$ or 0 dB.

Chapter 4

Optical injection locking

Optical injection locking (OIL) and optical phase locked loops (OPLL) are two methods of obtaining laser synchronization which have found wide range of applications [33].

Due to simpler implementation and high coherent light regeneration, OIL is chosen over OPLL in most applications. Today OIL is mostly used in applications such as carrier recovery for coherent detection in homodyne receivers, pump recovery in phase sensitive amplifiers, modulation bandwidth enhancement of lasers such as vertical cavity surface emitting lasers (VCSEL), chaos synchronizations, frequency transfer applications for atmoic clocks, meteorology and many more [34–37]. Since injection locking dynamics can be fairly complex, we focus only on the basic mechanism and its properties in this chapter.

When light from a high coherent laser, called the master laser is injected into a low coherent slave laser, the slave cavity is forced to follow master frequency and its phase. Hence the slave output will ideally be an exact replica or regenerated version of injected master. For locking to take place, it is a necessary that the free running frequencies of both the lasers are in proximity, which is decided by a parameter called locking bandwidth and this will be discussed a little later.

Usually OIL is described by a pulling mechanism where the injected master light pulls the slave cavity to oscillate at the master frequency. This theory was first described in RF oscillators by Adler [38] in 1946 where the locking of an oscillator circuit with external RF signal injection was shown. The behaviour of pulling is first demonstrated in optical domain by Stoven and Stier in 1966 [39] where they performed locking using two He-Ne Fabry-Perot lasers. Historically among all lasers, semiconductor lasers are most widely chosen for injection locking because of insufficient

frequency stability and large spectral linewidth. Whereas master lasers are chosen to be having very narrow linewidth with high frequency stability such as fiber lasers.

The pulling strength of injection locking also depends on locking bandwidth, given by the following equation under steady state condition [40]:

$$\Delta\omega_{LB} = \sqrt{1+\alpha^2} f_d \sqrt{\frac{P_{inj}}{P_{sl}}} \tag{4.1}$$

where f_d is the longitudinal mode spacing of the slave laser, α is the linewidth enhancement factor of the slave laser, P_{inj} is the injected master power and P_{sl} is the slave output power. The ratio of injected master power to the slave output power P_{inj}/P_{sl} is called the injection ratio and is an important parameter to approximate the locking bandwidth.

Locking bandwidth can be intuitively understood as the maximum allowed free running frequency difference between master and slave lasers in order to achieve locking. However, it is not necessary that stable locking can be performed even if the master and slave laser frequencies present with in the locking bandwidth. The plot in the Fig. (4.1) shows the optical injection ratio vs detuning frequency. The space between two solid lines where the unlocked regions share boundary is the locking bandwidth, which increases with increase in injection ratio. The region outside the locking bandwidth is "unlocked region" where stable locking cannot be performed or a periodic locking and unlocking takes place.

The unstable region inside the locking bandwidth is called the injection locking induced pulsations (ILIP) region where slave laser shows dynamically unstable behaviour with pulsations close to relaxation frequency leading to unstable locking. Hence there exists a narrow region where stable locking can be performed. It is important that, the master and slave frequencies should be very close and stable such that their frequency difference lies within the stable region especially when operated at extremely low injection ratios such as -75 dB discussed in paper (B).

When OIL is stably locked, under steady state condition the locked slave output experiences a phase shift corresponding to the free running frequency difference between master and slave given by [40]

$$\Delta\phi_L = -\sin^{-1}\left(\frac{\omega_m - \omega_{sl}}{\Delta\omega_{LB}}\right) - \tan^{-1}\alpha \tag{4.2}$$

Here $\omega_m - \omega_{sl}$ is the free running frequency difference between master and slave lasers and $\Delta\omega_{LB}$ is the locking bandwidth. The phase shift increases with decrease in locking bandwidth and at lower injection ratios this phase shift becomes very large. α is a constant depends on the laser material

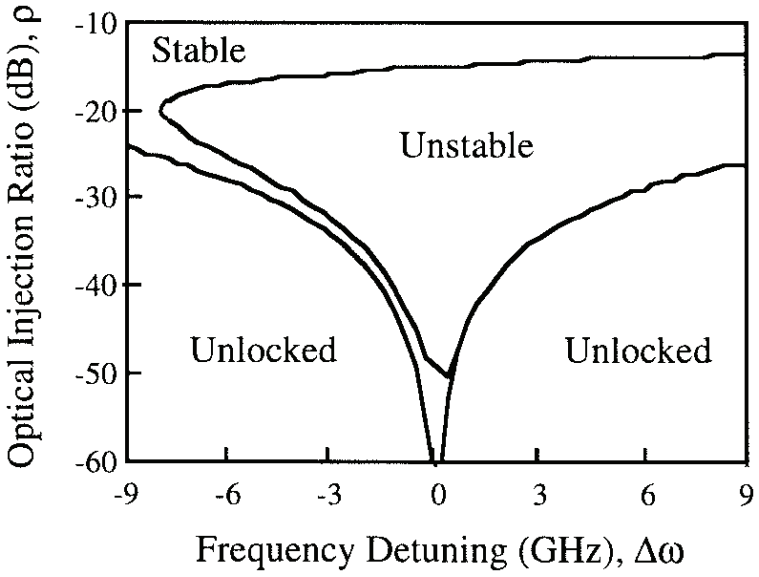

Figure 4.1: Locking characteristics of a semiconductor DFB laser [41]

property. The locked phase dependence property has been used in phase modulation applications where the phase is changed by modulating the drive current of the slave laser which eventually modulates the frequency of slave [42]. This equation is crucial for understanding the phase noise generated by OIL at low injection ratios, discussed in paper (B).

4.1 Phase locked loop

Due to thermal drifts of the slave and the master laser, the free running frequencies may drift up to typically few 10s of MHz. To perform injection locking when the locking bandwidth is much lower than the drift bandwidth, an external phase locked loop (PLL) is required. The operation and performance of such a phase locked loop is explained in paper (B). The basic principle behind the OIL PLL is that, the injection locked phase ϕ_L can be obtained at the slave laser output and the frequency drift is calculated using Eq. (4.2) and it is compensated by modulating the slave laser current.

Chapter 5

Practical implementation of PSA for free space communication

In free-space communication, low noise EDFAs are considered as pre-amplifiers at the receiver to amplify the received signal. If a PSA is used instead of EDFA, the transmitter should also be modified in order to satisfy the requirements of PSA as a pre-amplifier. Fig. (5.1) shows the implementation of PSA in a free space transmission link.

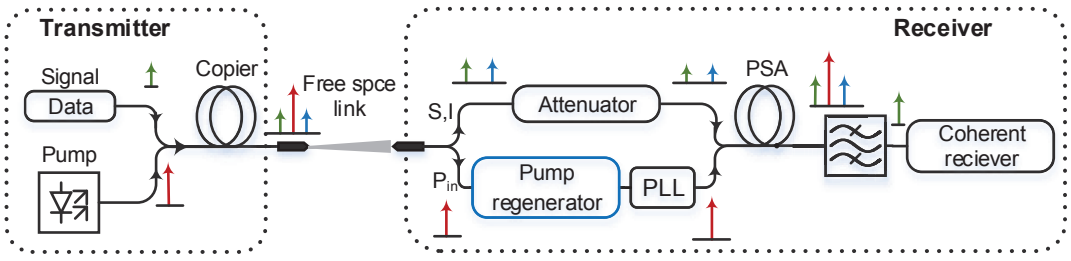

Figure 5.1: Set up for PSA implementation in a free space transmission link

5.1 Free space link with PSA receiver

5.1.1 Transmitter

Unlike EDFA, a PSA needs signal and idler waves as input to achieve a noise figure close to 0 dB quantum limit. Hence it is necessary that both the waves are generated in the transmitter. A copier stage combines the data modulated signal and pump waves from different laser sources in a HNLF where they interact due to four wave mixing to generate the idler. Copier is a 240 m length HNLF having a nonlinear coefficient $11(Wkm)^{-1}$. It is important that the input signal and pump polarisation are aligned for maximum conversion efficiency of FWM. The wavelengths of signal and pump is chosen according to the phase matching condition in the HNLF for PSA, will be discussed little later.

Correlated quantum noise is generated at the output of copier stage in both signal and the idler wavelengths due to FWM. Since the signal and idler are attenuated by large amounts in the free space channel, uncorrelated quantum noise dominates over the correlated noise from copier. Hence we can use the noise figure expressions are given by Eq. (3.21) in chapter 3.

5.1.2 Receiver

In reality, the recieved pump power for performing PSA is not considered in sensitivity calculation,whereas in free space communication all the power that is sent over the link needs to accounted. It is possible to generate phase coherent pump in the receiver without being transmitted through the channel, but it requires a part of received signal and idler waves power [43]. This will reduce the signal and idler power available for PSA and hence the sensitivity degrades. Transmitting the pump along with signal and idler would be necessary to avoid the sensitivity degradation. However, if the received pump comparable to signal and the idler power, the sensitivity can again be degraded due to presence of the pump.

In order to maintain the maximum sensitivity benefit of 3 dB over EDFA based receiver, the received pump power must be negligible compared to the signal and the idler power levels. Typical receivers for free space communications operate with sensitivities of few photons per bit. For PSA receiver to have sensitivities of few photons per bit, pump should contribute only a fraction of photons per bit. To get a clear understanding, in paper A we demonstrated that PSA based receiver sensitivity (signal+idler power) at BER = 10^{-3} is close to -50 dBm and in order to maintain this sensitivity the received pump should be -65 dBm or lower.

Injection locking at such low powers is a challenging task. We investigated different techniques to perform OIL at such lower powers, discussed in detail in paper (B).

In the receiver, the pump is separated from signal and the idler waves using a WDM coupler for regeneration using OIL. The regenerated pump wave is amplified and combined with signal and idler in a HNLF stage for PSA. Fiber chosen for PSA is a 4 stage HNLF spools with lengths 103m,128m,164m and 204m spliced with isolators in between the spools to reduce the stimulated brillouin scattering threshold. Each HNLF is spooled by straining the fiber with a linear strain across the length so as to increase the Brillouin threshold further [27] . All the HNLFs are manufactured and strained by OFS Denmark. Straining the fiber allowed the Brillouin threshold to be 27 dBm also the zero dispersion wavelength changes to 1543 nm from 1542 nm. The maximum pump power that can be injected into the PSA is 27 dBm resulting in maximum parametric gain of 18 dB. As discussed in chapter 3 the pump wavelength should be in anomalous dispersion region to have maximum gain, we chose pump wavelength to be 1554.13 nm and the signal wavelength at 1550.65 nm in a region where maximum signal exponential gain can be achieved.

To achieve the maximum phase sensitive gain, the relative phase of all the waves at the input of should be constant $\theta_{rel} = \phi_p - \phi_s - \phi_i = \pi/2$ as discussed in chapter 3. The paths of signal-idler and pump are different before reaching the PSA makes the phase of the pump change randomly with respect to signal-idler. We employ a phase locked loop (PLL) to maintain the relative phase between signal, idler and pump to achieve maximum signal gain at the output. A small fraction of signal output of PSA is fed as input to the PLL, which then is sampled digitally in a micro-controller and compared to gain of previous sample. The difference in samples voltage is converted to optical phase change and compensated in pump path using a PZT such that maximum signal gain is maintained.

The phase in-sensitive gain was 18 dB whereas phase sensitive gain was close to 24 dB. Due to the large losses in free space, PSA input signal powers can be as low as -60 dBm resulting in output only -36 dBm which is insufficient for receiver as receiver thermal noise can dominate the signal. Hence signal is amplified with an EDFA immediately after PSA with sufficient gain.

The signal is received using a coherent receiver and data is captured using real time scope. The data is post processed off-line with digital signal processing algorithms, starting with I-Q imbalance compensation then equalization followed by frequency and phase estimation and compensation.

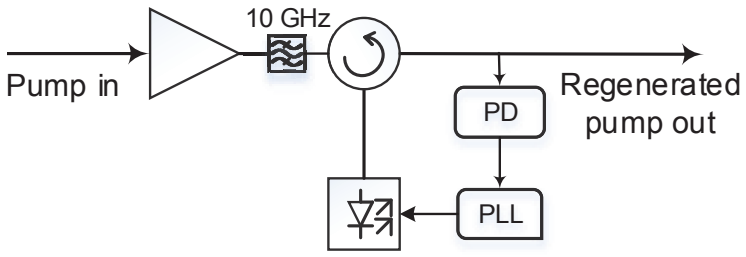

Figure 5.2: Injection locking with PLL

5.1.3 Optical injection locking

A brief theory of optical injection locking is discussed in chapter 3. When it comes to practical implementation for free space communication, it becomes challenging as the sensitivity of PSA requires pump powers to be as low as -65 dBm or below. At this low powers, the locking bandwidth is less than 10 MHz.

Fig. 5.2 shows the injection locking set up for pump recovery stage in the PSA. An EDFA is used as pre amplifier to amplify the low power pump, the filter is used to amplify the ASE generated in the pump and then a PLL along with OIL is used to perform locking stably.

Note that, the PLL used for stabilizing OIL is different from PLL used for maintaining relative phase of the pump, signal and the idler phases for maximum PSA gain.

5.2 Challenges in implementation

There are many other challenges in implementing PSA to achieve such low sensitivity and there are some practices that needs to be taken care, which will be discussed here.

- PSA operation depend on the coherent interaction of signal and idler, therefore sensitive to polarisation, relative phase of these waves. Hence it is important that these properties are maintained constant to achieve maximum gain.
- Since the pump is split from signal and idler path for regeneration using injection locking, the relative phases of the waves in different paths can drift due to thermal and acoustic noise. A phase locked loop implemented to maintain the relative phase between signal, idler and pump to achieve maximum signal gain in all times. When

the input signal powers into PSA are quite low, corresponding optical signal to noise ratio (OSNR) $<$ 5dB, the operation of PLL is not optimal at such low powers. This is improved by filtering the signal after PSA with very narrow band filter (22 GHz) by blocking out most of the noise and also by changing the PLL parameters, such as increasing sampling rate and dither frequency although doing this degrades sensitivity by a small amount.

- Another challenge is stable optical injection locking at low powers as the stable locking region can be very narrow. Challenge here is to keep the free running slave frequency stable without sudden drifting because of thermal, vibrational noise in the lab or polarisation drifts in the pump which may cause OIL to unlock.

Chapter 6

Conclusions and future outlook

In this work, we have shown that phase sensitive amplifier can be used as a pre-amplifier for free-space communication. Although PSA requires three waves at the input, PSA can have almost 3 dB better in sensitivity compared to an EDFA based receiver. To achieve this, the important challenge was to receover the pump from sub nano watt powers, which was done using phase-locked loop and EDFA pre-amplifier. This allowed to operate the PSA without any sensitivity penalty due to the presence of received pump. We believe this method is a better choice of pump regeneration instead of complicated method chosen for regeneration at the receiver stage [43] as it require part of signal and idler power. In paper (A) we have shown a sensitivity of 4.5 photons per bit including the pump power.

In the future, we would like to study the minimum sensitivity that one can achieve by using PSA by studying the mutual information of the received signal. This could give some information on how far we are from the Shannon's capacity and how low sensitivity we can achieve. Of course this require injection locking to operate at even lower power levels. To successfully demonstrate such lower sensitive receiver for free space links with error free transmission, we should also implement forward error correction codes.

Chapter 7

Summary of papers

Paper A

"High Sensitivity Receiver Demonstration Using Phase Sensitive Amplifier for Free-Space Optical Communication" Proceedings of European Conference on Optical Communications(ECOC), Paper. Tu.2.E.3, 2017.

In this paper, we demonstrated a record sensitivity of 4.5 photons per bit of using phase sensitive amplifier based receiver for free-space communication. This involves operating injection locking based pump recovery at powers as low as -62 dBm. The experiment was extended to atmospheric channel where turbulence was included in the channel by using a rotating turbulence phase plate emulating turbulence for 1 km free-space link in the lab. Results show that PSA sensitivity can be 3 dB and 1.3 dB better than EDFA when the channel is free-space without and with turbulence.

My contribution I developed the idea, performed the experiment together with Vijayan, I wrote the paper.

Paper B

"Optical injection locking at sub nano-Watt powers", *accepted for publication in optics letters.*

The sensitivity of a PSA based receiver can be degraded mainly due to the presence of pump at the receiver input. To have a negligible penalty due to the pump, the received pump power needs to much lower than signal and idler powers. So, we need to perform injection locking at power below -65 dBm.
In this paper, we discuss the methods we have implemented for stable injection locking at powers as low as -65dBm. A phase locked loop was employed to keep the locking stable at low powers and an EDFA pre-amplifier was used to lock at even low powers by amplifying the input. An interesting conclusion from this paper is that, using a EDFA pre-amplifier we can reduce the phase noise at the locked output rather than increasing it. We also found that the injection locking phase noise depends on the slave linewidth and that can increase with decreasing injection ratio.
We have used such a low power injection locking in PSA based receiver environment and observed a penalty of 0.4 dB relative to the case with high power pump and no injection locking, due to phase noise generated in injection locking.

My contribution I developed the idea, performed the experiment and wrote the paper.

References

[1] H. Hemmati, *Deep space optical communications*. John Wiley & Sons, 2006, vol. 11.

[2] D. Abraham, "Future mission trends and their implications for the deep space network," in *Space 2006*, 2006, p. 7247.

[3] D. M. Boroson, B. S. Robinson, D. V. Murphy, D. A. Burianek, F. Khatri, J. M. Kovalik, Z. Sodnik, and D. M. Cornwell, "Overview and results of the lunar laser communication demonstration," in *Free-Space Laser Communication and Atmospheric Propagation XXVI*, vol. 8971. International Society for Optics and Photonics, 2014, p. 89710S.

[4] D. M. Cornwell, "Nasa's optical communications program for 2017 and beyond," in *2017 IEEE International Conference on Space Optical Systems and Applications (ICSOS)*. IEEE, 2017, pp. 10–14.

[5] E. Agrell and M. Karlsson, "Power-efficient modulation formats in coherent transmission systems," *Journal of Lightwave Technology*, vol. 27, no. 22, pp. 5115–5126, 2009.

[6] A. Ludwig, M.-L. Schulz, P. Schindler, S. Wolf, C. Koos, W. Freude, and J. Leuthold, "Stacked modulation formats enabling highest-sensitivity optical free-space links," *Optics express*, vol. 23, no. 17, pp. 21 942–21 957, 2015.

[7] C. Gobby, Z. Yuan, and A. Shields, "Quantum key distribution over 122 km of standard telecom fiber," *Applied Physics Letters*, vol. 84, no. 19, pp. 3762–3764, 2004.

[8] N. Bertone, R. Biasi, and B. Dion, "Overview of photon counting detectors based on cmos processed single photon avalanche diodes (spad), ingaas apds, and novel hybrid (tube+ apd) detectors," in *Semiconductor Photodetectors II*, vol. 5726. International Society for Optics and Photonics, 2005, pp. 153–164.

[9] M. D. Eisaman, J. Fan, A. Migdall, and S. V. Polyakov, "Invited review article: Single-photon sources and detectors," *Review of scientific instruments*, vol. 82, no. 7, p. 071101, 2011.

[10] J. Katz, "The 2.5 bit/detected photon demonstration program: Phase 2 and 3 experimental results," 1982.

[11] A. Ishimaru, *Wave propagation and scattering in random media*. John Wiley & Sons, 1999, vol. 12.

[12] L. C. Andrews and R. L. Phillips, *Laser beam propagation through random media*. SPIE press Bellingham, WA, 2005, vol. 152.

[13] Y. Ren, H. Huang, G. Xie, N. Ahmed, Y. Yan, B. I. Erkmen, N. Chandrasekaran, M. P. Lavery, N. K. Steinhoff, M. Tur *et al.*, "Atmospheric turbulence effects on the performance of a free space optical link employing orbital angular momentum multiplexing," *Optics letters*, vol. 38, no. 20, pp. 4062–4065, 2013.

[14] P. Polynkin, A. Peleg, L. Klein, T. Rhoadarmer, and J. Moloney, "Optimized multiemitter beams for free-space optical communications through turbulent atmosphere," *Optics letters*, vol. 32, no. 8, pp. 885–887, 2007.

[15] R. Stolen, "Phase-matched-stimulated four-photon mixing in silica-fiber waveguides," *IEEE Journal of Quantum Electronics*, vol. 11, no. 3, pp. 100–103, 1975.

[16] R. Stolen and J. Bjorkholm, "Parametric amplification and frequency conversion in optical fibers," *IEEE Journal of Quantum Electronics*, vol. 18, no. 7, pp. 1062–1072, 1982.

[17] J. Armstrong, N. Bloembergen, J. Ducuing, and P. Pershan, "Interactions between light waves in a nonlinear dielectric," *Physical review*, vol. 127, no. 6, p. 1918, 1962.

[18] N. M. Kroll, "Parametric amplification in spatially extended media and application to the design of tuneable oscillators at optical frequencies," *Physical Review*, vol. 127, no. 4, p. 1207, 1962.

[19] R. Gadonas, A. Marcinkevičius, A. Piskarskas, V. Smilgevičius, and A. Stabinis, "Travelling wave optical parametric generator pumped by a conical beam," *Optics communications*, vol. 146, no. 1-6, pp. 253–256, 1998.

[20] C. M. Caves, "Quantum limits on noise in linear amplifiers," *Phys. Rev. D*, vol. 26, pp. 1817–1839, Oct 1982.

[21] J. A. Levenson, I. Abram, T. Rivera, and P. Grangier, "Reduction of quantum noise in optical parametric amplification," *JOSA B*, vol. 10, no. 11, pp. 2233–2238, 1993.

[22] W. Imajuku, A. Takada, and Y. Yamabayashi, "Low-noise amplification under the 3 db noise figure in high-gain phase-sensitive fibre amplifier," *Electronics Letters*, vol. 35, no. 22, pp. 1954–1955, 1999.

[23] C. McKinstrie and S. Radic, "Phase-sensitive amplification in a fiber," *Optics express*, vol. 12, no. 20, pp. 4973–4979, 2004.

[24] Z. Tong, C. Lundström, P. Andrekson, C. McKinstrie, M. Karlsson, D. Blessing, E. Tipsuwannakul, B. Puttnam, H. Toda, and L. Grüner-Nielsen, "Towards ultrasensitive optical links enabled by low-noise phase-sensitive amplifiers," *Nature Photonics*, vol. 5, no. 7, p. 430, 2011.

[25] R. Slavík, F. Parmigiani, J. Kakande, C. Lundström, M. Sjödin, P. A. Andrekson, R. Weerasuriya, S. Sygletos, A. D. Ellis, L. Grüner-Nielsen *et al.*, "All-optical phase and amplitude regenerator for next-generation telecommunications systems," *Nature Photonics*, vol. 4, no. 10, p. 690, 2010.

[26] S. L. Olsson, H. Eliasson, E. Astra, M. Karlsson, and P. A. Andrekson, "Long-haul optical transmission link using low-noise phase-sensitive amplifiers," *Nature communications*, vol. 9, no. 1, p. 2513, 2018.

[27] G. P. Agrawal, "Nonlinear fiber optics," in *Nonlinear Science at the Dawn of the 21st Century*. Springer, 2000, pp. 195–211.

[28] T. Schneider, *Nonlinear optics in telecommunications*. Springer Science & Business Media, 2013.

[29] K. Hill, D. Johnson, B. Kawasaki, and R. MacDonald, "cw three-wave mixing in single-mode optical fibers," *Journal of Applied Physics*, vol. 49, no. 10, pp. 5098–5106, 1978.

[30] N. Shibata, R. Braun, and R. Waarts, "Phase-mismatch dependence of efficiency of wave generation through four-wave mixing in a single-mode optical fiber," *IEEE Journal of Quantum Electronics*, vol. 23, no. 7, pp. 1205–1210, 1987.

[31] J. Hansryd, P. A. Andrekson, M. Westlund, J. Li, and P.-O. Hedekvist, "Fiber-based optical parametric amplifiers and their applications," *IEEE Journal of Selected Topics in Quantum Electronics*, vol. 8, no. 3, pp. 506–520, 2002.

[32] C. J. McKinstrie, S. Radic, and M. Raymer, "Quantum noise properties of parametric amplifiers driven by two pump waves," *Optics Express*, vol. 12, no. 21, pp. 5037–5066, 2004.

[33] M. R. Stiglitz, "Highly coherent semiconductor lasers," *Microwave Journal*, vol. 36, no. 9, pp. 192–193, 1993.

[34] B. Dahmani, L. Hollberg, and R. Drullinger, "Frequency stabilization of semiconductor lasers by resonant optical feedback," *Optics letters*, vol. 12, no. 11, pp. 876–878, 1987.

[35] Z. Ahmed, H. Liu, D. Novak, Y. Ogawa, M. Pelusi, and D. Kim, "Locking characteristics of a passively mode-locked monolithic dbr laser stabilized by optical injection," *IEEE Photonics Technology Letters*, vol. 8, no. 1, pp. 37–39, 1996.

[36] C.-H. Chang, L. Chrostowski, and C. J. Chang-Hasnain, "Injection locking of vcsels," *IEEE Journal of Selected Topics in Quantum Electronics*, vol. 9, no. 5, pp. 1386–1393, 2003.

[37] Z. G. Pan, S. Jiang, M. Dagenais, R. A. Morgan, K. Kojima, M. T. Asom, R. E. Leibenguth, G. D. Guth, and M. W. Focht, "Optical injection induced polarization bistability in vertical-cavity surface-emitting lasers," *Applied physics letters*, vol. 63, no. 22, pp. 2999–3001, 1993.

[38] R. Adler, "A study of locking phenomena in oscillators," *Proceedings of the IRE*, vol. 34, no. 6, pp. 351–357, 1946.

[39] H. Stover and W. Steier, "Locking of laser oscillators by light injection," *applied physics letters*, vol. 8, no. 4, pp. 91–93, 1966.

[40] F. Mogensen, H. Olesen, and G. Jacobsen, "Locking conditions and stability properties for a semiconductor laser with external light injection," *IEEE Journal of Quantum Electronics*, vol. 21, no. 7, pp. 784–793, 1985.

[41] J. Yao, "Microwave photonics," *Journal of Lightwave Technology*, vol. 27, no. 3, pp. 314–335, 2009.

[42] S. Kobayashi and T. Kimura, "Optical phase modulation in an injection locked algaas semiconductor laser," *Electronics Letters*, vol. 18, no. 5, pp. 210–211, 1982.

[43] Y. Okamura, K. Kondo, S. Seki, Y. Ohmichi, M. Koga, and A. Takada, "Frequency nondegenerate optical parametric phase-sensitive amplifier repeater by using recovered pump carrier generated from phase-conjugated twin waves," in *Optical Fiber Communications Conference and Exhibition (OFC), 2016.* IEEE, 2016, pp. 1–3.